

# Femtosecond Photoionization of Atoms under Noise

Kamal P. Singh and Jan M. Rost

*Max Planck Institute for the Physics of Complex Systems,  
Nöthnitzer Strasse 38, 01187 Dresden, Germany.*

We investigate the effect of incoherent perturbations on atomic photoionization due to a femtosecond mid-infrared laser pulse by solving the time-dependent stochastic Schrödinger equation. For a weak laser pulse which causes almost no ionization, an addition of a Gaussian white noise to the pulse leads to a significantly enhanced ionization probability. Tuning the noise level, a stochastic resonance-like curve is observed showing the existence of an optimum noise for a given laser pulse. Besides studying the sensitivity of the obtained enhancement curve on the pulse parameters, such as the pulse duration and peak amplitude, we suggest that experimentally realizable broadband chaotic light can also be used instead of the white noise to observe similar features. The underlying enhancement mechanism is analyzed in the frequency-domain by computing a frequency-resolved atomic gain profile, as well as in the time-domain by controlling the relative delay between the action of the laser pulse and noise.

PACS numbers: 02.50.Ey, 42.50.Hz, 32.80.Rm

## I. INTRODUCTION

The role of noise on driven quantum systems is a subject of considerable interest and importance. Several studies exist in the literature on this broad topic. For instance, the noise-induced effects in the nanoscale quantum devices such as Josephson junctions [1, 2], the macroscopic phase transitions due to quantum fluctuations [3], driven multilevel quantum systems under incoherent environment [4], and stochastic ionization of Rydberg atoms by microwave noise [5], to mention just a few. In these examples, the action of noise on a system can be broadly classified as being of two types: either of destructive nature, i.e., noise must be avoided; or of constructive nature necessitating its presence.

It is this nontrivial latter aspect of noise-induced effects that has been subject of intense investigation [1, 2, 6, 7]. In particular, the stochastic resonance phenomenon (SR) provides a paradigm for the constructive role of noise in nonlinear classical as well as quantum systems [7]. The essence of quantum SR is the existence of an optimum amount of noise in a nonlinear system that enhances its response to a weak coherent input forcing [8, 9, 10, 11]. Despite the diversity of nonlinear dynamics exploiting classical SR, most of the quantum mechanical studies of the effect have focused on the so-called spin-Boson model, which provides an analog of a classical double-well potential [1, 2, 12, 13]. However, many other physical systems exist, particularly atoms or molecules exposed to strong laser pulses, where the quantum dynamics can be nonlinear and therefore added noise could play an important role.

The presence of noise is also worth studying from the point of view of steering quantum dynamics of atomic or molecular systems [14, 15, 16]. Traditionally this is achieved with strong, tailored laser pulses by exploiting their nonperturbative and nonlinear interaction with the atomic systems. In this context, it has been shown that weak noise of various origin in multilevel ladder systems

plays a crucial role [14]. Many scenarios have been discussed, such as the need to either cooperate or fight with de-coherence in the closed-loop control [17], and to engineer the environment to achieve the steering of quantum systems towards a desired state [18]. In the same spirit, white shot noise has been used to dissociate diatomic molecules [19]. This has implications for the field of quantum control. Motivated by the concept of exploiting noise in nonlinear systems, one can ask the question if noise can serve as an extra tool for quantum control. Indeed, the concept of the quantum SR effect has not been exploited for additional insight in controlling the quantum phenomenon.

In this article, we provide a detailed study of the influence of noise in a generic quantum situation, namely the photoionization of a single-electron atom interacting with an ultrashort laser pulse. We will demonstrate the conditions under which a resonance-like behavior emerges in the stochastic photoionization process. This noise-induced phenomenon is studied for a variety of laser pulses, from a few optical cycles duration to very long ones, and of varying intensities. Furthermore, we suggest the experimental observability of the effect by employing a broadband chaotic light instead of white Gaussian noise. Lastly, we characterize the underlying gain-mechanism in the frequency-domain in order to identify the crucial frequency-bands in the broad noise spectrum.

The article is organized as follows. Section II introduces our model of the simplest atom interacting with a femtosecond laser pulse and white noise, and describes our method to solve its stochastic Schrodinger equation. In section III, we show the results of the ionization probability (IP) for various combinations of the laser pulse and noise. The existence of a stochastic resonance-like behavior is quantified using an enhancement factor which is computed from IP. The sensitivity of this noise-induced effect is tested with laser pulses of varying duration and strength, and other types of noise such as a realizable broadband chaotic light. To characterize

the enhancement mechanism, we compute the frequency-resolved gain profile of the driven atom, and study the role of relative time-delay between noise and the laser pulse. Finally, section IV provides a summary of results with our conclusions.

## II. DESCRIPTION OF THE MODEL

### A. Hydrogen atom interacting with a laser pulse and noise

We consider as an example the simplest single-electron atom, i.e., the hydrogen atom. Due to the application of an intense linearly polarized laser field  $F(t)$ , the electron dynamics is effectively confined in one-dimension along the laser polarization axis [20]. The Hamiltonian for such a simplified description of the hydrogen atom, which is here also perturbed by a stochastic force  $\xi(t)$  [21], reads as (atomic units,  $\hbar = m = e = 1$ , are used unless stated otherwise),

$$H(x, t) = \frac{\hat{p}^2}{2} + V(x) + x\{F(t) + \xi(t)\}, \quad (1)$$

where  $x$  is the position of the electron and  $\hat{p} = -i \partial/\partial x$  is the momentum operator. The external perturbations,  $F(t)$  and  $\xi(t)$ , are dipole-coupled to the atom. The potential is approximated by a non-singular Coulomb-like form,

$$V(x) = -\frac{1}{\sqrt{x^2 + a^2}}. \quad (2)$$

Such a soft-core potential with parameter  $a$  has been routinely employed to study atomic dynamics in strong laser fields [22]. It successfully describes many experimental features of multiphoton or tunnel ionization [20], and the observation of the plateau in higher harmonic generation spectra [22].

The laser field is a nonresonant mid-infrared (MIR) femtosecond pulse described as,

$$F(t) = f(t)F_0 \sin(\omega t + \delta). \quad (3)$$

Here  $F_0$  defines the peak amplitude of the pulse,  $\omega$  denotes the angular frequency, and  $\delta$  is the carrier-envelope phase. We choose a smooth pulse envelop  $f(t)$  of the form,

$$f(t) = \begin{cases} \sin^2(\pi t/(2\tau)), & t < \tau \\ 1, & \tau \leq t \leq T_p - \tau \\ \cos^2(\pi(t + \tau - T_p)/(2\tau)), & T_p - \tau < t \leq T_p, \end{cases}$$

where  $T_p$  is the pulse duration and  $\tau$  the time for turning the field on and off.

The noise term  $\xi(t)$  is a zero-mean Gaussian white noise having the following properties,

$$\langle \xi(t) \rangle = 0, \quad (4)$$

$$\langle \xi(t)\xi(t') \rangle = 2D \delta(t - t'), \quad (5)$$

and noise intensity  $D$  [23].

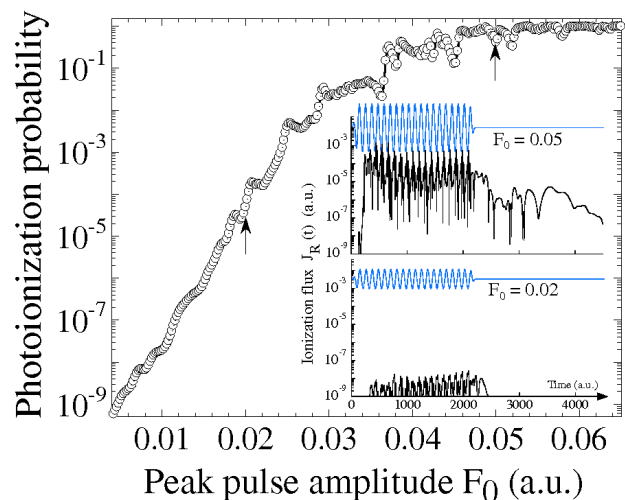


FIG. 1: The ionization probability  $P_I$  as a function of the laser peak amplitude  $F_0$ . Insets show the ionization flux versus time for two different pulses (top parts of curves) of amplitudes,  $F_0 = 0.05$  and  $F_0 = 0.02$ , marked by arrows on IP curve. Here  $\omega = 0.057$ ,  $\delta = 0.0$ ,  $T_p = 20\pi/\omega$  and  $\tau = 2\pi/\omega$ .

### B. Stochastic quantum dynamics

The presence of the stochastic forcing term in the Hamiltonian as described above, makes the quantum evolution nondeterministic. Thus an averaging over a large number of realizations of the stochastic force is required in order to produce a statistically meaningful solution of the following time-dependent stochastic Schrödinger equation,

$$i \frac{\partial \Psi(x, t)}{\partial t} = H(x, t) \Psi(x, t). \quad (6)$$

For a given realization, the numerical solution of the Schrödinger equation amounts to propagating the initial wave function  $|\Psi_0\rangle$  using the infinitesimal short-time stochastic propagator,

$$U_\xi(\Delta t) = \exp\left(-i \int_t^{t+\Delta t} H(x, t) dt\right). \quad (7)$$

One can compute  $U_\xi(\Delta t)$  using the split-operator fast Fourier algorithm [24]. Details of the method employed are described in the Appendix. Successive applications of the stochastic propagator  $U_\xi(\Delta t)$  advance  $|\Psi_0\rangle$  forward in time.

Note that the initial state  $|\Psi_0\rangle$  is always chosen to be the *ground state* of the system having an energy of  $I_b = -0.5$  a.u.. This is obtained by the imaginary-time relaxation method for  $a^2 = 2$  [20]. To avoid parasitic reflections of the wavefunction from the grid boundary, we employ an absorbing boundary [24].

The ionization flux leaking in the continuum on one side, is defined as [25],

$$J_R(x_R, t) = \text{Re}[\Psi^* \hat{p} \Psi]_{x_R}, \quad (8)$$

where  $x_R$  is a distant point (typically 500 a.u.) near the absorbing boundary. The ionization rate is integrated over a sufficiently long time interval to obtain the corresponding total ionization probability,

$$P = \int_0^\infty J_R(x_R, t) dt. \quad (9)$$

In the following section, we shall use both the ionization flux, and the photoionization yield, to study the interplay between the laser pulse and noise. From the point of view of stochastic resonance-like phenomena, we aim at establishing the constructive role of noise in atomic photoionization due to a femtosecond laser pulse.

### III. RESULTS

#### A. Optimal stochastic enhancement of photoionization

##### 1. Photoionization as a nonlinear effect

Let us first consider the response of the atom interacting with a short but strong laser pulse only. Fig. 1 shows the ionization probability  $P_I$  versus the peak pulse amplitude  $F_0$  for a 20 cycle long MIR laser pulse ( $\omega = 0.057$ ). This figure shows that with increasing values of  $F_0$  the ionization probability first increases nonlinearly, and then saturates to the maximum value of unity, for  $F_0 > 0.05$ . The behavior of  $P_I(F_0)$  is a characteristic signature for many atomic and molecular systems interacting with nonresonant intense laser pulses [22].

The laser pulse produces (nonlinear) ionization of the atom which is most easily understood, especially in the time domain, with the picture of a periodically changing tunneling barrier. Ionization flux is produced close to those times when the effective potential  $U(x, t) = V(x) + xF(t)$ , is maximally bent down by the dipole-coupled laser field. This is illustrated in the inset of Fig. 1 with the temporal evolution of the ionization flux for laser pulses (shown in the top parts of inset) with two different peak amplitudes  $F_0 = 0.05$  and  $F_0 = 0.02$  (see arrows in Fig. 1). Time-resolved ionization peaks separated by the optical period ( $2\pi/\omega$ ) are clearly visible for both peak field amplitudes. In addition,  $J_R(t)$  shows a complex interference pattern [inset of Fig. 1] due to the modulated Coulomb barrier for  $F_0 = 0.05$ . However, quite strikingly, if  $F_0$  is reduced to 0.02 a.u., the ionization flux collapses by around five orders of magnitude as shown in Fig. 1. One can therefore conclude that the photoionization dynamics is highly nonlinear, and in particular it exhibits a form of “threshold” dynamics where the threshold is created by the condition for over-the-barrier ionization.

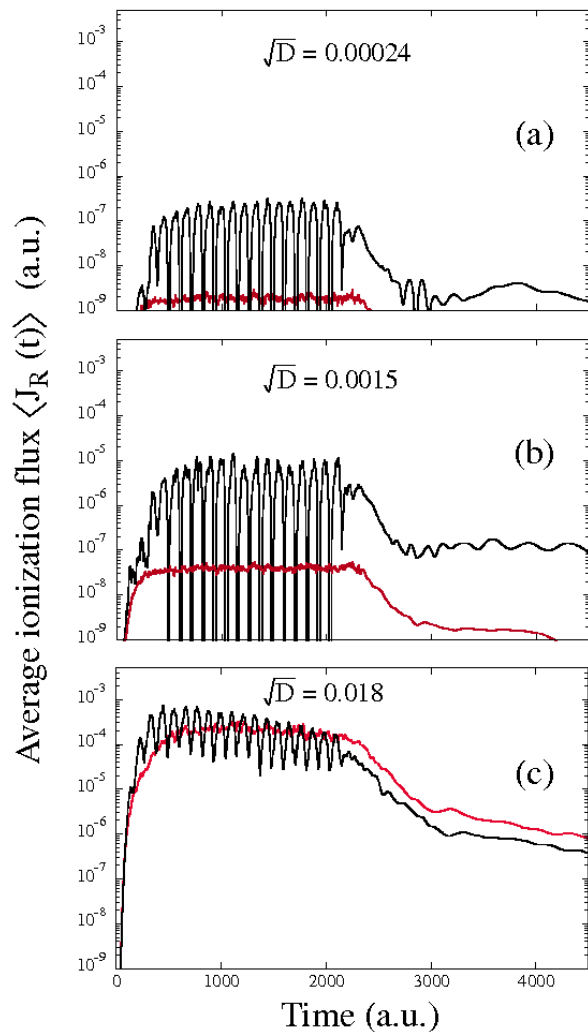


FIG. 2: Ionization flux for a weak laser pulse  $F_0 = 0.02$ , with three values of noise amplitude, (a)  $\sqrt{D} = 0.00024$ , (b) 0.0015, and (c) 0.018. Background featureless curves (red) show the corresponding purely noise-driven ( $F_0 = 0$ ) flux. The flux is averaged over 50 realizations.

##### 2. Ionization induced by noise alone

Here we look into the possibility of efficiently ionizing the atom, when it is subjected to white Gaussian noise only. The interaction time of the atom with the noise is kept identical to the laser pulse duration  $T_p$  (see inset of Fig. 3). Fig. 2 shows the evolution of the ionization flux  $\langle J_R(t) \rangle$  which is averaged over 50 different realizations of the noise. One can see that for small noise amplitudes the ionization flux exhibits a featureless curve, producing the ionization flux around  $10^{-9}$ . As the noise level is increased, the featureless ionization curve rises monotonically as shown in Fig. 2(a)-(c). By integrating the stochastic ionization flux, one can compute the corresponding ionization probability  $P_n$ , which is simply equal

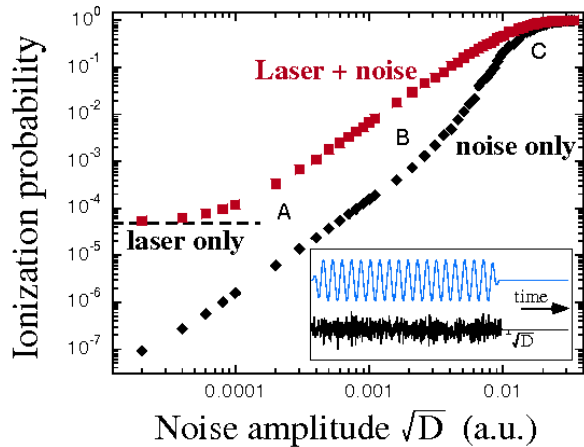


FIG. 3: The ionization probability versus the noise amplitude  $\sqrt{D}$  for the noise alone  $P_n$  (diamonds) and for the laser pulse ( $F_0 = 0.02$ ) with noise  $P_{l+n}$  (squares). The points A-C corresponds to the three cases considered in Fig. 2. The dashed line shows the limit of vanishing noise, i.e., the probability due to the laser pulse alone  $P_l$ . Inset: an example of laser pulse and noise

to the area under the curve  $\langle J_R(t) \rangle$ . The resulting noise-induced ionization probability  $P_n$  versus the noise amplitude is shown in Fig. 3. As can be seen the stochastic ionization probability rises monotonically with the noise level. For ultra-intense noise, such that its strength becomes comparable to the atomic binding field, obviously full ionization can be achieved. We should mention that similar effects have been observed in other systems, for example, the purely noise-induced molecular dissociation [19], and the ionization induced by weak noise of the highly excited Rydberg atoms [5]. However, in our case we consider the atom to be initially in its ground state.

Although the application of noise alone, or the laser pulse alone, can lead to the atomic ionization, we aim to study whether a combination of both the laser pulse and noise makes the ionization process more efficient as compared to the individual cases.

### 3. Simultaneous application of the laser pulse and noise

We have seen that the atomic photoionization due to an intense femtosecond laser pulse is a highly nonlinear quantum phenomenon, and in particular, the ionization response collapses for a “weak” laser pulse (see inset of Fig. 1). Motivated by the quantum SR effect, we wish to explore if the noise can recover the strong periodic ionization flux for the weak laser pulse. To answer this question, in Fig. 2(a) we show the average ionization flux when a small noise of amplitude,  $\sqrt{D} = 0.00024$ , is added to the previously weak laser pulse ( $F_0 = 0.02$ ). Note that the atomic excitation time by the laser and the noise here are identical. One can see that for such a feeble noise amplitude, the periodic structure in atomic

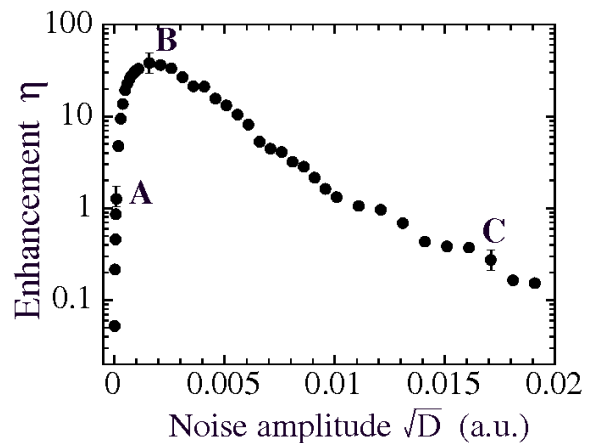


FIG. 4: The enhancement in photoionization due to quantum SR. The points marked A-C correspond to the noise amplitudes of Fig. 2(a)-(c), respectively. At point B the ratio  $\sqrt{D_{opt}}/F_0 = 0.075$ . The error bars indicate the standard deviation of  $\eta$  calculated using more than 1000 different noise realizations.

ionization gets enhanced by more than one order of magnitude, as compared to the case of the noise alone which is shown as the background featureless curve. Hence, the observed net enhancement can be attributed to a nonlinear quantum interaction between the coherent pulse and noise.

As the noise level is further increased, we observe an enhancement of the periodic ionization profile by around three orders of magnitude as shown in Fig. 2(b). However, the increase in noise level also causes the background structureless stochastic ionization curve to rise monotonically. For strong noise (Fig. 2(c)), these periodic structures tend to wash out and the process is effectively controlled by the noise. Hence one expects, the existence of an intermediate noise level where the nonlinear ionization is optimally enhanced.

The net enhancement of the atomic ionization due to interplay between the laser pulse and the noise can be characterized by the enhancement factor [21],

$$\eta = \frac{P_{l+n} - P_0}{P_0}, \quad (10)$$

with  $P_0 = P_l + P_n$ . Although this is different compared to the quantifiers commonly used [1, 2],  $\eta$  is more suitable for our case. One can verify that a zero value of  $\eta$  corresponds to the case when either the laser pulse ( $P_l \gg P_n$ ) or the noise ( $P_l \ll P_n$ ) dominates. In Fig. 4, we have plotted the enhancement factor  $\eta$  versus the noise amplitude  $\sqrt{D}$ . It exhibits a sharp rise, followed by a maximum at a certain value of the noise (point B), and then a gradual fall off. It is worth mentioning that only a modest noise-to-laser ratio ( $\sqrt{D_{opt}}/F_0 = 0.075$ ) is required to reach the optimum enhancement (here  $\eta_{max} = 36$ ).

Before investigating other properties of the enhancement effect, it is worth making three remarks. First,

although the enhancement curve bears striking resemblance to the typical SR curve, it is not SR effect where the matching of the time scales between coherent and incoherent driving exists. The underlying gain mechanism here is completely different, as we shall see later. One can perhaps call this as a generalized quantum SR for such atomic systems, in the sense of the existence of an optimum noise level. Second, the location of the optimum enhancement is governed by an empirical condition, when the strengths of the laser pulse and noise are comparable, in terms of the ionization flux produced by their individual action  $P_l \sim P_n$ . This can be verified in Fig. 3 for the enhancement curve shown in Fig. 4. Third, due to the presence of the random noise term in the Hamiltonian, the optimal solution is only statistically unique. We have computed the standard deviation of the enhancement factor  $\eta$  using 1000 realizations,  $\sigma = \sqrt{\langle \eta^2 \rangle - \langle \eta \rangle^2}$ . The corresponding  $\sigma$  values are shown by error bars on the  $\eta$  curve in Fig. 4.

#### 4. Enhancement curves for a variety of laser pulses

In this subsection, we study the sensitivity of the stochastic enhancement curves on the laser pulse. In particular, we study the role of two parameters: (i) the pulse duration  $T_p$ , and (ii) the peak pulse amplitude  $F_0$ . In Fig. 5, we have plotted enhancement curves versus the noise amplitude for pulses of fixed amplitude ( $F_0 = 0.02$ ) but of varying durations from 5 to 30 optical cycles. One can clearly see that, the enhancement features (particularly the location and strength of the optima) are robust for pulses ranging from ultrashort few cycle duration to quite long ones.

Although we do not show, we have also verified that variation in the carrier envelop phase  $\delta$  of the laser pulse  $F(t)$  [see Eq. (3)] does not modify the enhancement effect. This can be expected due to the presence of the noise term, by which any effect of  $\delta$  is averaged out. Furthermore, we have also observed similar enhancement curves for other forms of the pulse envelop, such as  $f(t) = \sin^2(\pi t/T_p)$ .

To investigate the dependence of  $\eta$  on the laser pulse amplitude  $F_0$ , we choose some moderate noise amplitude value, for example,  $\sqrt{D} = 0.0015$ . For this fixed  $\sqrt{D}$ , we now increase the peak pulse amplitude  $F_0$  of the 20 cycles pulse from zero to a large value, and calculate the IP for each value of  $F_0$ . The obtained probabilities for different cases are plotted in Fig. 6(a), which are then used to compute the enhancement factor  $\eta$  in Fig. 6(b). Here,  $\eta$  also exhibits a nonmonotonic feature versus the laser peak amplitude, thus suggesting a range of  $F_0$  where the addition of noise can be useful. This dependency is intuitively explained. Since for weak laser pulse the process is dominated by the noise and the  $\eta$  collapses. On the other hand, if the laser peak amplitude is too strong (comparable to over-the-barrier ionization threshold), the pulse can ionize the atom by itself, and the noise has no role

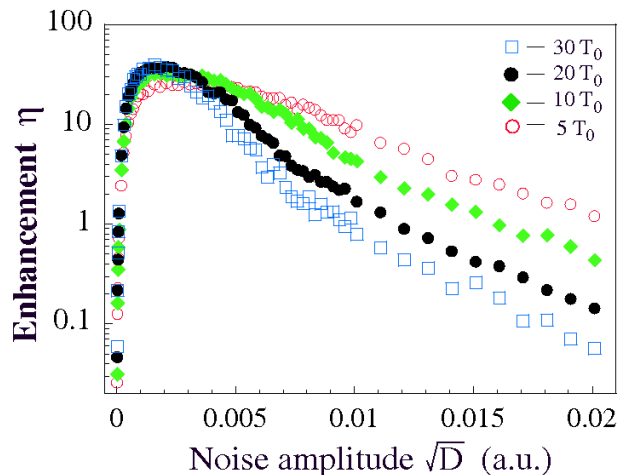


FIG. 5: The enhancement factor versus the noise amplitude for four different values of pulse durations  $T_p$ : 5, 10, 20, 30 optical period  $T_0$ . Here  $F_0 = 0.02$ , and other parameters are the same as in previous figures.

to play. Thus, it is for the intermediate values of the noise and laser pulse amplitudes, where this nonlinear enhancement mechanism can be significant. From Figs. 4 and 6, one can conclude that in order to maximize the net ionization yield, a particular pair of  $F_0$  and  $\sqrt{D}$  is required.

## B. Employing chaotic light instead of the white noise

### 1. Generation and characterization of chaotic light

To experimentally observe this effect, the most challenging task is the generation of intense white noise. For instance, if one considers the thermal radiation from a blackbody (such as the sun) as a possible source of the white noise, its noise intensity falls short by many orders of magnitude [26], compared to the one required for the optimum of Fig. 4. We thus look into alternatives for generating a noise-like waveform. One possibility is to employ modern pulse shaping techniques, whereby one can design waveforms of almost arbitrary shapes [27, 28]. To realize such a chaotic light, we choose a large number of frequency modes,  $N$ , in a finite but broad bandwidth  $\Delta\omega$ . These modes can be, for example, different Fourier components of an ultrashort laser pulse. The total electric field  $Z(t)$  is a sum of these  $N$  individual modes as [29],

$$Z(t) = \sqrt{\frac{2}{N}} \sum_{n=1}^N F_{rms} \sin(\omega_n t + \phi_n), \quad (11)$$

where  $\omega_n$ ,  $\phi_n$  denote the angular frequency, phase of  $n^{\text{th}}$  mode, respectively; and  $F_{rms}$  is the root-mean-square amplitude of  $Z(t)$ . Note that here we consider

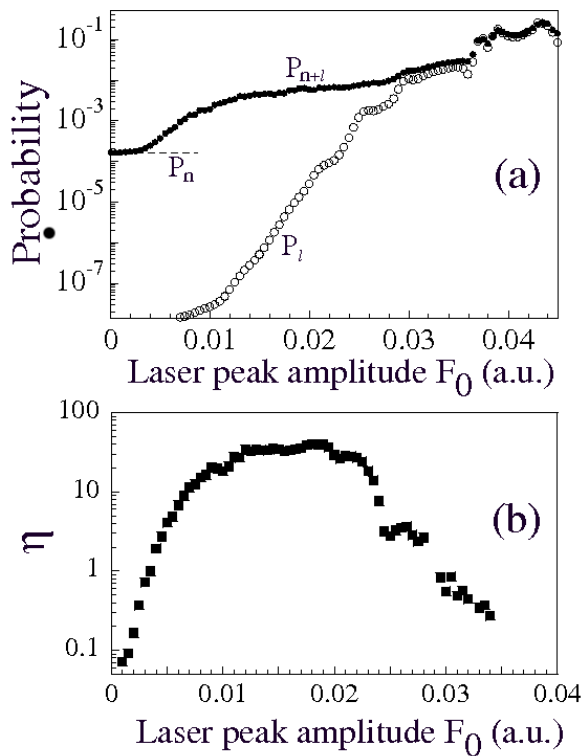


FIG. 6: The dependence of enhancement on  $F_0$  for a fixed noise amplitude  $\sqrt{D} = 0.0015$ . (a) Ionization probabilities versus  $F_0$  for laser only  $P_l$ , and for laser with noise  $P_{l+n}$ . The dashed line shows the limiting value of  $P_n$ . (b) The enhancement vs  $F_0$  curve obtained from the probability curves shown in (a).

these frequency modes to oscillate independently with their phases  $\phi_n$  assuming random values relative to each other. In this particular case of phase-randomized coherent modes, the total field  $Z(t)$  at any point will be noise-like, fluctuating in intensity due to the interference between modes. Inset in Fig. 7 shows an example of such a chaotic light spectrum for  $N = 1024$  in a chosen bandwidth (BW) of 0.75 (corresponding to a 32 attosecond pulse) [30]. Such a construct tends to the white noise, in the limit of  $\Delta\omega, N \rightarrow \infty$ . In the following subsection, we consider a simultaneous application of the weak laser pulse and chaotic light (instead of the white noise) and see if the enhancement effect can be preserved.

### 2. Photoionization by the chaotic light

When we replace white noise by the chaotic light (BW=0.75 and  $N = 1024$ ), one can see in Fig. 7 that most of the features of the enhancement phenomenon remain intact. In particular, the intensity and location of the optimum is very close to the one obtained for the white noise case in Fig. 4. We also recover other features of the enhancement mechanism with the chaotic

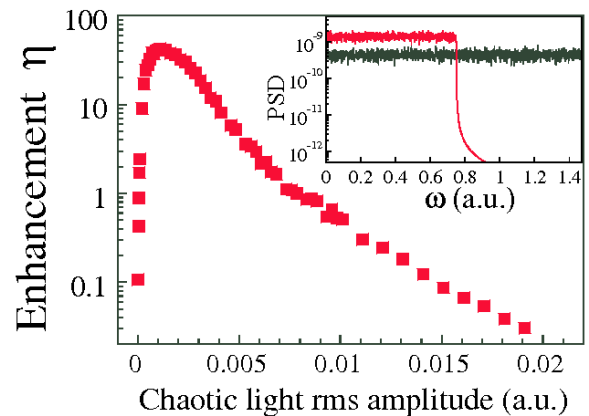


FIG. 7: Enhancement induced by a broadband chaotic light. The peak amplitude and frequency of the 20 cycle laser pulse are  $F_0 = 0.02$  and  $\omega = 0.057$ , respectively. The bandwidth of chaotic light is  $\Delta\omega = 0.75$  with central frequency  $\omega_0 = 0.375$ . Inset: power spectral density (PSD) of the chaotic light compared to the one for the white noise.

light such as its dependence on the pulse duration  $T_p$  and pulse amplitude  $F_0$ .

This observation not only suggests the possibility of observing the effect using a finite but broadband chaotic light, but also raises the question concerning the relevant frequency components in the chaotic light spectrum, to be discussed next.

## C. Spectral and temporal analysis of the gain mechanism

### 1. Frequency-resolved gain profile

In this subsection, we will analyze the mechanism of stochastic enhancement in both, the frequency domain and time domain. In particular, we aim to identify frequency components in the broad spectrum of noise (or chaotic light) which are the crucial ones to provide the gain. For this purpose, we compute a frequency-resolved atomic gain (FRAG) profile using a pump-probe type of setting as described below.

It is well known that when an atom interacts linearly with a weak external field, the energy absorption takes place at its resonant frequencies. However, due to its interaction with a strong laser pulse, the unperturbed atomic states are significantly modified leading to a completely different frequency response of the driven atom. Indeed, such a modified spectral response is the relevant quantity when the atom is also subjected to noise. So, how can one measure precisely the frequency resolved gain  $G(\nu)$  offered by the atom? One possible way to observe FRAG is to consider the previously employed laser pulse ( $\omega = 0.057$ ,  $F_0 = 0.02$ ) as a pump pulse and replace noise by a tunable monochromatic probe pulse,  $F_p(t) = f(t)F_p \sin(\omega_p t)$ . The probe amplitude  $F_p$  is much

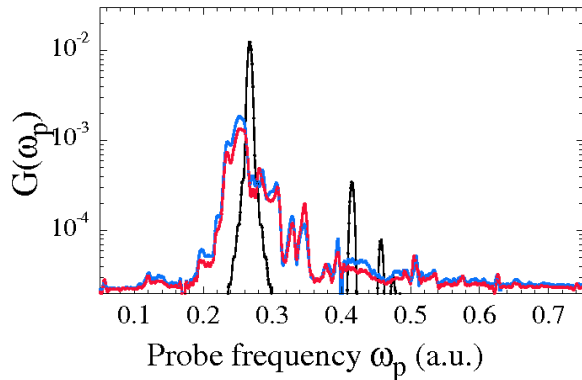


FIG. 8: Frequency-resolved gain  $G(\omega_p)$  of the atom which is driven by a 10 cycle laser pulse of  $F_0 = 0.02$  at  $\omega = 0.057$ . The atomic gain is probed by a simultaneous application of a weak probe beam  $F_p = 0.0002$  of tunable frequency  $\omega_p$ . Both, the depletion of the ground state population (blue) and the net absorption of energy (red) due to the probe are plotted. The gain of driven atom is also compared with the bare atomic gain (black).

weaker than the driving laser pulse [ $F_p/F_0 = 0.01$ ], such that it does not significantly alter the quasi energy levels, but can drive transitions between them. For an atom prepared in its ground state, a FRAG profile is obtained by measuring either the depletion of the ground state population or the net energy absorption, as a function of the probe frequency  $\omega_p$ .

Such a gain profile  $G(\omega_p)$  is shown in Fig. 8 for the atom driven by a 10 cycle long laser pulse of amplitude  $F_0 = 0.02$ . Although the FRAG shows lots of structure, the dominant peaks appear around the first atomic transition frequency. A closer inspection of Fig. 8 reveals that there is a dip at the unperturbed resonance frequency  $\omega_{01} = 0.267$ . The main peak is indeed shifted beyond the linear Stark shift for our model. These shifts and broadening of the atomic resonances are caused by the strong laser pulse, since the field can drive the electron significantly away from the nucleus leading to strong nonlinear perturbation to its bound states. Such a FRAG curve provides a fingerprint of the atomic gain under the strong laser pulse. The frequency bands that correspond to the peaks in the obtained gain curve are indeed the most useful ones to obtain the enhancement. In the following, we will test the validity of this statement by designing a chaotic light where significant resonance frequencies are filtered from its spectrum.

## 2. Chaotic light with missing resonant frequencies

To show that the useful frequencies are *not* simply the resonant frequencies of the atom, we have designed a chaotic light spectrum perforated by digging holes in its spectral density around the first few atomic transition frequencies. As can be seen from Fig. 9, almost no en-

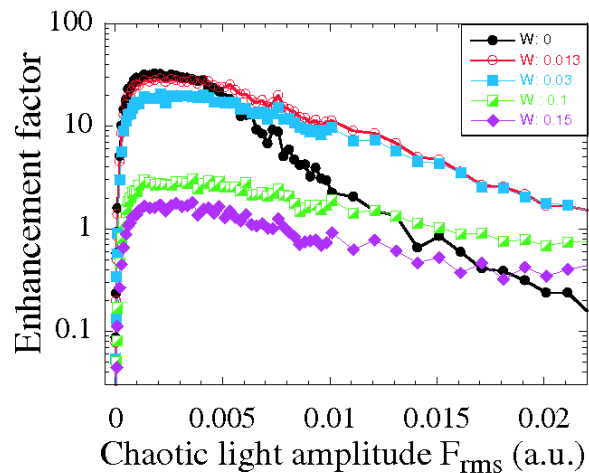


FIG. 9: Enhancement curves due to chaotic light spectrum perforated by holes at the first three resonance frequencies. Difference curves correspond to the increasing hole widths of  $w = 0.0, 0.013, 0.03, 0.1$  and  $0.15$ .

hancement is lost, if the hole width  $w$  is below  $0.013$  a.u., which already includes the linear ac stark shift of the atomic states. However, by increasing the hole width such that no frequency component exists in the noise spectrum where the FRAG has dominant peaks leads to a collapse of the enhancement mechanism, as shown in Fig. 9. This observation validates the importance of FRAG structure in identifying the useful spectral bands in noise. It suggests that for the simultaneous presence of the laser pulse and noise, non-resonant frequency components are the dominant ones.

It is worth making few remarks here. First, the FRAG is a property of the atom interacting with a particular strong laser pulse. Thus, the detailed features of the gain curve depends on both the atomic system and on the laser pulse parameters. But this doesn't affect the general conclusion drawn from such a curve. Second, it is also possible to obtain the enhancement using a monochromatic beam instead of the chaotic broadband light, if its frequency is properly tuned to the new "resonances". But, the advantage of using a broadband source is that the enhancement becomes independent of both, the particular atom and the FRAG structure for different pulse parameters.

## 3. Role of relative delay between signal and noise

Up to now we have considered the case of a perfect synchronization, i.e., a simultaneous application of the laser pulse and noise to observe the enhancement. We now wish to relax this synchronization constrain between the laser pulse and noise to test if the enhancement still exists. Such a scenario would not only help the experimental search of similar effects, but also provides an alternative aspect of the enhancement mechanism as compared

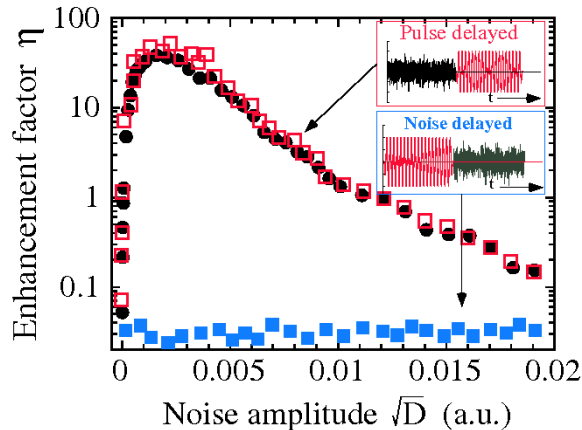


FIG. 10: Enhancement factor  $\eta$  versus the noise amplitude  $\sqrt{D}$  for various cases, application of noise first and then the laser pulse (empty squares), application of laser pulse first and then noise (filled square), simultaneous application of laser and noise (circles). Insets depicts schematically temporal signal applied to the atom for corresponding cases.

to the one mentioned above.

There are two possible ways to expose the atom to a laser pulse and noise sequentially: (i) the atom first interacts with noise only and then we apply the laser pulse, or conversely, (ii) the laser pulse is applied first and then the noise is applied. Note that for both cases, there is no direct interplay between laser and noise. The enhancement factor  $\eta$ , which is defined as before, is shown in Fig. 10 for both the cases. One can clearly see that for the case-(i)  $\eta$  curve looks very similar to the one for simultaneous action of laser and noise. But for the case-(ii), the enhancement curve collapses.

Although we obtain almost identical enhancement curves for cases of, first-noise then laser pulse and simultaneous action of noise with laser pulse, the gain providing frequency components are fundamentally different in each case. The gain curves for both cases are given in Fig. 8. For the sequential application of noise and laser, the atomic gain is basically at the resonant frequencies of the unperturbed atom. Thus the resonant frequencies (particularly the first few) are the most fertile ones in the noise spectrum. In this case, a two-step picture of the enhancement mechanism applies, where the atom first absorbs energy from the noise leading to an exponential population distribution, and the laser causes ionization from “noise-heated” atom in a second step.

#### IV. SUMMARY AND CONCLUSION

We have investigated photoionization of a hydrogen atom which is subjected to both, a MIR femtosecond laser pulse and white Gaussian noise. Due to the inherent nonlinearity of the ionization process, a form of quantum stochastic resonance-like behavior has been ob-

served. This quantum SR leads to a dramatic enhancement (by several orders of magnitude) in the nonlinear ionization when a specific but small amount of white noise is added to the weak few cycle laser pulse. We have further shown the signatures of the enhancement effect for different types of the laser pulses from a few cycles to few tens of cycles duration. Moreover, if the noise amplitude is kept fixed to some level, and the peak pulse amplitude is varied, again a curve with a specific maximum is obtained for the enhancement parameter. These results suggest the existence of an optimum combination of the laser pulse and noise, if one is interested in optimizing the relative ionization enhancement. The same effect is also achieved if one uses realizable broadband chaotic light instead of white noise. We emphasize that the effect is robust with respect to a range of experimentally accessible parameters such as the pulse duration.

The enhancement mechanism is analyzed in the frequency domain by measuring the frequency-resolved gain profile of the atom under a strong laser pulse, employing a pump-probe type of setting. The gain providing frequencies are significantly modified from the unperturbed atomic resonances, suggesting the non-resonant nature of the noise absorption. However, if we introduce a relative time-delay between the laser pulse and noise the enhancement is still present, provided the noise acts first on the atom. In this case, the useful frequencies in the noise spectrum are at the atomic resonances.

Finally, analogous effects are also expected in other systems provided the following three conditions are fulfilled: (i) The system has a single-well finite binding potential with multiple energy levels, (ii) it can be subjected to a (nonresonant) coherent optical driving, and (iii) it can be subjected to an incoherent perturbation. Since these conditions are sufficiently general, other systems (SQUIDS, molecules etc) might also display similar features [31, 32].

#### Acknowledgments

We thank A. Kenfack, W. Peijie, N. Singh, A. Buchleitner, and P. Hänggi for fruitful discussions.

#### APPENDIX

In this appendix we briefly present an algorithm for the numerical simulation of the time-dependent stochastic Schrödinger equation, Eq. (6) in the text, where the Hamiltonian is given by Eq. (1). The properties of the white Gaussian noise  $\xi(t)$  are defined in Eq. (4)-(5). Our basic approach is to use the split-operator fast-Fourier transform (SOFFT) method due to Feit and Fleck (which is well known for the deterministic case) [25], and adapt it to the case when the Hamiltonian contains an additional stochastic term  $\xi(t)$ .



Recalling briefly that if there were no random term, the solution of Eq. (6) can be obtained by defining the standard propagator  $U(t_0, t)$ , which when applied on initial state wavefunction  $|\Psi_0\rangle$  propagates it forward in time. The usual approach to compute the solution of the Schrödinger equation is to discretize the total propagation time into  $N$  small steps of equal intervals  $\Delta t$ . The resulting exact short-time propagator can be written as,

$$U_\xi(\Delta t) = \exp\left(-i \int_t^{t+\Delta t} (H_{det}(x, t) + x\xi(t)) dt\right). \quad (\text{A-1})$$

Here,  $H_{det}(x, t) = \hat{p}^2/2 + V(x) + xF(t)$ , is the deterministic atomic Hamiltonian including the laser-atom interaction term. In order to incorporate the white noise term within the framework of SOFFT method, one can rewrite the propagator as,

$$U_\xi(\Delta t) = U(\Delta t) \exp\left(-i \int_t^{t+\Delta t} x\xi(t) dt\right), \quad (\text{A-2})$$

where,  $U(\Delta t) = \exp(-iH_{det}(x, t)\Delta t)$ , denotes the deterministic part of the propagator. The stochastic integral in the exponential can be interpreted in the Stratonovitch sense [23] using the properties of the white Gaussian noise as follows,

$$\int_t^{t+\Delta t} \xi(t) dt = \sqrt{2D\Delta t} X_t, \quad (\text{A-3})$$

where  $X_t$  is a random number having Gaussian distribution and of unit variance. This makes the propagator a stochastic operator. Note that even in the presence of

the noise term the operator is unitary, i.e., it preserves the norm of the wavefunction.

One can approximate the exact propagator given by Eq. (A-2) following a three-step splitting leading to the following expression,

$$U_\xi(\Delta t) = \exp\left(-i\frac{p^2}{2}\Delta t\right) \exp(-iV_\xi(x, t)\Delta t) \exp\left(-i\frac{p^2}{2}\Delta t\right), \quad (\text{A-4})$$

with,  $V_\xi(x, t) = V(x) + xF(t) + \sqrt{2D/\Delta t}X_t$ . Note that the effect of noise is simulated by inserting at every time step a random number  $X_t$  whose statistical properties are described above. The right hand side of Eq. (A-4) is thus equivalent to the free propagation over a half time increment  $\Delta t/2$ , a random phase change from the action of potential  $V_\xi(x, t)$  over the whole time  $\Delta t$ , and an additional free particle propagation over  $\Delta t/2$ .

This operator splitting is correct up to second order in the time step  $\Delta t$  for the noise-free part, but due to the stochastic integration it is accurate up to only first-order for the stochastic part. In the actual calculation  $\Delta t$  is chosen sufficiently small, such that a further reduction in its value does not alter the accuracy of the physical results. For a given realization of the random number sequence entering in the propagator via  $X_t$ , one generates a quantum ‘‘trajectory’’ for the wavefunction. To extract the physical observable, an ensemble average of the desired quantity over a large number of noise realizations is needed. Other simulation parameters such as the grid size and the grid resolutions should be taken as described in the literature [24].

- 
- [1] L. Gammaitoni, P. Hänggi, P. Jung, and F. Marchesoni, *Rev. Mod. Phys.* **70**, 223 (1998).
  - [2] T. Wellens, V. Shatokhin, and A. Buchleitner, *Rep. Prog. Phys.* **67**, 45 (2004).
  - [3] M. Greiner, O. Mandel, T. Esslinger, T.W. Hansch, and I. Bloch, *Nature* **415**, 39 (2002).
  - [4] H. Rabitz *et al.*, *Science* **288**, 824 (2000).
  - [5] R. Blumel *et al.*, *Phys. Rev. Lett.* **62**, 341 (1989); J. G. Leopold and D. Richards, *J. Phys. B* **24**, L243 (1991); L. Sirko *et al.*, *Phys. Rev. Lett.* **71**, 2895 (1993).
  - [6] R. L. Badzey and P. Mohanty, *Nature* **437**, 995 (2005).
  - [7] K. Wiesenfeld and F. Moss, *Nature* **373**, 33 (1995).
  - [8] R. Löfstedt and S. N. Coppersmith, *Phys. Rev. Lett.* **72**, 1947 (1994).
  - [9] A. Buchleitner and R. N. Mantegna, *Phys. Rev. Lett.* **80**, 3932 (1998).
  - [10] S. F. Huelga and M. B. Plenio, *Phys. Rev. A* **62**, 052111 (2000).
  - [11] L. Viola, E. M. Fortunato, S. Lloyd, C.-H. Tseng, and D. G. Cory, *Phys. Rev. Lett.* **84**, 5466 (2000).
  - [12] D. E. Makarov and N. Makri, *Phys. Rev. B* **52**, R2257 (1995).
  - [13] M. Grifoni and P. Hänggi, *Phys. Rev. Lett.* **76**, 1611 (1996).
  - [14] Ian Walmsley and H. Rabitz, *Phys. Today*, Aug. **43** (2003).
  - [15] E. D. Potter *et al.*, *Nature* **355**, 66 (1992).
  - [16] A. Assion *et al.*, *Science* **282**, 919 (1998).
  - [17] A. Pechen and H. Rabitz *Phys. Rev. A* **73**, 062102 (2006).
  - [18] F. Shuang and H. Rabitz *J. Chem. Phys. A* **124**, 154105 (2006).
  - [19] A. Kenfack and J. M. Rost, *J. Chem. Phys.* **123**, 204322 (2005).
  - [20] M. Protopapas *et al.*, *Rep. Prog. Phys.* **60**, 389 (1997); J. Javanainen, J. H. Eberly and Q. Su, *Phys. Rev. A* **38**, 3430 (1988).
  - [21] Kamal P. Singh and Jan M. Rost *Phys. Rev. Lett.* **98**, 160201 (2007).
  - [22] G. Mainfray and C. Manus, *Rep. Prog. Phys.* **54**, 1333 (1991).
  - [23] C. Gardiner, *Handbook of Stochastic Processes* (Springer-Verlag, Berlin, 1983).
  - [24] J. A. Fleck, J. R. Moris, and M. D. Feit, *Appl. Phys.* **10**, 129 (1976).
  - [25] C. Cohen-Tannoudji, B. Diu, and F. Laloë, *Quantum Mechanics, Vol. I* (Springer-Verlag, Berlin, 1983).

- [26] R. C. Dunbar and T. B. McMahon, *Science* **279**, 194 (1998).
- [27] D. Yelin, D. Meshulach, and Y. Silberberg, *Opt. Lett.* **22**, 1793 (1997).
- [28] T. Witte, D. Zeidler, D. Proch, K. L. Kompa, and M. Motzkus *Opt. Lett.* **27**, 1793 (2002).
- [29] A. M. Weiner, *Rev. Scien. Instrument* **71**, 1929 (2000).
- [30] R. L. Martens *et al.*, *Phys. Rev. Lett.* **94**, 033001 (2005).
- [31] S. Chelkowski *et al.*, *Phys Rev. Lett.* **65**, 2355 (1990); A. Assion *et al.*, *Science* **282**, 919 (1998).
- [32] A. Wallraff, T. Duty, A. Lukashenko, and A. V. Ustinov, *Phys. Rev. Lett.* **90**, 037003 (2003).